

Vibrational Energy Distribution of SiO Produced via the Chemical Activation of SiH_3OH

Atsuko Takahara,[#] Ryuta Araki, Atsumu Tezaki,[*] and Hiroyuki Matsui[##]

Department of Mechanical Engineering, The University of Tokyo, Hongo, Bunkyo-ku, Tokyo 113

(Received October 20, 2000)

Vibrationally excited SiO has been observed in the 193 nm photolysis of N_2O/SiH_4 mixtures with and without great excess of H_2. While $SiH_4 + O(^1D)$ (1) has been known to produce SiO in the mixture without H_2, present kinetic analyses of SiO and OH indicate that $SiH_3 + OH$ (2) is responsible for the SiO production in the mixture with H_2. The observed nascent vibrational distributions, approximated by Boltzmann distributions of $T_v = 5200 \pm 660$ K for (1) and 2800 ± 790 K for (2), are reasonably accounted for by a statistical model assuming multi-step unimolecular decomposition of hot silanol.

Relatively extensive studies have been conducted on a reaction $SiH_3 + O_2$,[1–4] which is recognized to be the most important initial step in the silane oxidation.[5–7] However, very little has been known about subsequent reactions of partially oxidized intermediates except the energetical information derived by ab initio theoretical studies.[8–12]

$SiH_3 + OH$ has been reported in our previous studies[13,14] to be one of the main product channels of $SiH_4 + O(^1D)$ reaction (branching fraction was determined as 0.24), in which inverted vibrational distribution of OH was observed. Although the non-statistical distribution has been frequently attributed to a direct abstraction pathway, $O(^1D)$ readily inserts into a Si–H bond of silane to form an activated silanol which then decomposes into various fragments. A notable feature of the $SiH_4 + O(^1D)$ reaction is the production of SiO as a result of the multiple-step unimolecular decomposition of the activated silanol;

$$SiH_4 + O(^1D) \rightarrow (SiH_3OH)^* \rightarrow SiO + 2H_2 \text{ and other products} \quad (1)$$

which is 575 kJ mol^{-1} exothermic for the production of SiO. A recent molecular beam study supports reaction 1 as the mechanism of SiO production, where the life time of the reaction intermediate SiH_3OH is long enough to ensure the isotropic angular distribution for SiO.[15] Reaction 1 is also supported by the fact that a simple quasi-static model can explain the observed nascent vibrational temperature of SiO (5200 K) and the product branching fraction to SiO (0.13). Since no such product as CO has been believed to be formed in the reaction of $CH_4 + O(^1D)$,[16] this is one of the distinct contrasts between the kinetics of silanes and of hydrocarbons.

It is indicated that chemically activated silanol is also produced by the recombination reaction of SiH_3 and OH,

$$SiH_3 + OH \rightarrow (SiH_3OH)^* \rightarrow SiO + 2H_2 \text{ and other products} \quad (2)$$

through our experimental examination using a laser photolysis of N_2O/SiH_4 mixtures with excess amounts of H_2. Although silanol produced via (2) has 234 kJ mol^{-1} less energy than that from $SiH_4 + O(^1D)$, it is still sufficiently energized to decompose into fragments such as $SiO + 2H_2$. The present study focuses on a comparison of the nascent internal energies of the product SiO starting at two considerably different energies of chemically activated silanol. The unimolecular decomposition dynamics of the activated silanol is then discussed based on the comparison of the product SiO vibrational distributions in the reactions (1) and (2). Such comparison will provide important information on the dynamics of the unimolecular decomposition of silanol.

Experimental

In this work, the time dependence of $OH(v = 0, 1)$ and $SiO(v)$ was monitored in the mixtures of SiH_4/N_2O/He with and without much excess addition of H_2. The experimental setup is the same as that used in our previous paper,[14] i.e., the reaction is initiated by an excimer laser photolysis in a quasi-static flow cell and time-dependent measurements for species concentrations are conducted by means of a LIF probe technique. A frequency-doubled optical parametric oscillator (OPO; Continuum, Surelite OPO) was used as the probe light source in UV region. SiO was detected at the $A^1\Pi$–$X^1\Sigma^+$ (v'–v'') transitions in the wavelength region 226–280 nm where bands of $v'' = 0$ to 8 are included. OH was detected at the $A^2\Sigma^+$–$X^2\Pi i$ (v'–v'') transitions of $1'$–$0''$ (282.5 nm) and $2'$–$1''$ (288.5 nm) bands. The linewidth of the UV beam ranged from 4 to 7 cm^{-1} and the typical fluence was 100 μJ mm^{-2}. No saturation was observed at this comparatively low spectral density.

Mixtures of N_2O, SiH_4 and H_2 with He carrier gas were flowed in the cell at room temperature (297 K), and were irradiated by 193 nm ArF excimer laser (Lambda Physik, Compex 102) pulses. Roughly 10^{-3} of N_2O is photodecomposed by the typical fluence

Present address: Institut für Physicalische Chemie, Universität Göttingen, Tammannstr. 6, D-37077, Göttingen, Germany.

Present adress: Department of Ecological Engineering, Toyohashi University of Science and Technology, Tempaku-cho, Toyohashi 441-8580.

(10 mJ cm^{-2}) of the photolysis laser at the observation point.

In the mixture of SiH_4/N_2O without H_2, the following reactions are responsible for the production of SiO:

$$N_2O + h\nu \rightarrow O(^1D) + N_2$$

$$SiH_4 + O(^1D) \rightarrow OH, SiO + \text{other products} \quad (1)$$

$$N_2O + O(^1D) \rightarrow \text{products}. \quad (3)$$

It is noted that in the reaction (1) a direct H-abstraction channel yielding $SiH_3 + OH$ is also included in the consideration of overall rate and product branching fractions, if present.

The addition of much excess of H_2 ensures the significant occurrence of $SiH_3 + OH$ through the following reaction sequence:

$$H_2 + O(^1D) \rightarrow OH + H \quad (4)$$

$$SiH_4 + OH \rightarrow SiH_3 + H_2O \quad (5)$$

$$SiH_4 + H \rightarrow SiH_3 + H_2 \quad (6)$$

$$SiH_3 + OH \rightarrow (SiH_3OH)^* \rightarrow SiO + 2H_2, \quad (2a)$$

$$SiH_3 + OH \rightarrow \text{other products} \quad (2b)$$

while reactions (1) and (3) are restricted to be negligible for the present experimental condition i.e., $k_4(H_2)/k_1(SiH_4) \gg 1$, and $k_4(H_2)/k_3(N_2O) \gg 1$. In the reaction (2b), a direct channel yielding $SiH_2 + H_2O$ should be included.

Time profiles of OH(v) and SiO(v) are compared between the cases with and without H_2 in the samples so that the kinetics of SiO formation is analyzed.

Results and Discussion

Time Profiles with and without H_2. Typical time profiles of SiO(v) and OH(v) are shown in Fig. 1 and Fig. 2, respectively. In the mixture of 300 mTorr N_2O/10 mTorr SiH_4 without H_2, both SiO and OH are promptly produced predominantly by the reaction of $SiH_4 + O(^1D)$. The reaction time constant is nearly 1 μs and the following rise of SiO(0) until ca. 200 μs is attributed to the vibrational relaxation from higher SiO(v) as previously investigated.[17] When an excess amount of H_2 is present, the profile of SiO turns remarkably different, i.e., the prompt generation decreased by about an order and the gradual rise extends to ca. 400 μs, although the maximum amount of SiO(0) is almost the same for the two cases. As for OH(0), addition of H_2 increases the prompt generation by 20 times, while the decay time constants are very close to those obtained in the absence of H_2.

The species concentration profiles have been simulated by means of a numerical integration of a detailed reaction mechanism. Whereas the reactions 1–6 dominate in this system as described in the previous section, minor secondary reactions were taken from the reported SiH_4 oxidation mechanism.[6] As summarized in Table 1, the rate constants of reactions (1), (3), (4) and (6) were taken from the cited literature and the rate constant for (2) and its product branching fraction to SiO, indicated as ϕ, were varied. The rate constant for (5) was also treated as an adjustable parameter.

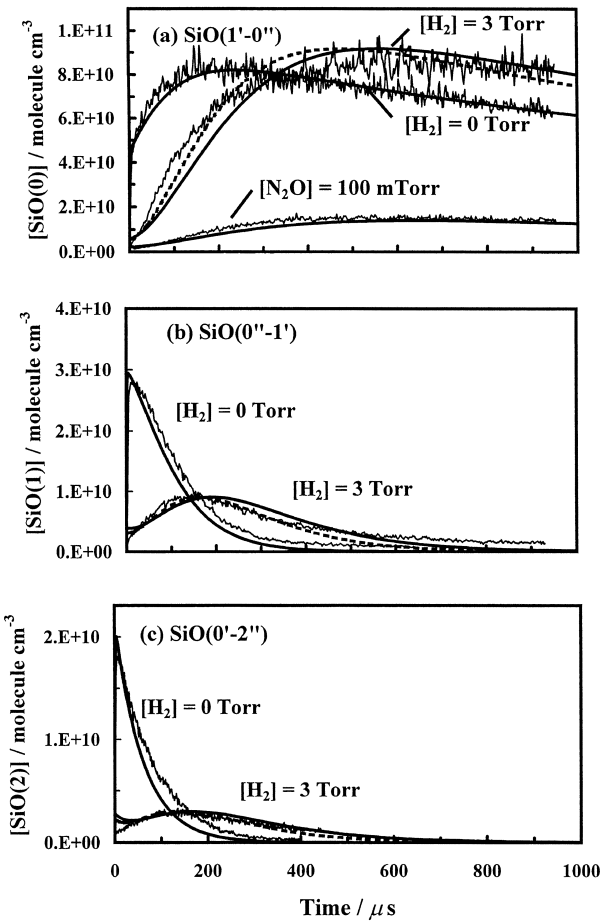

Fig. 1. Time profiles of SiO(v) in the 193 nm photolysis of N_2O/SiH_4 mixtures with and without H_2. (a) $v = 0$ probed at 230.1 nm (1′–0″ band); (b) $v = 1$ at 241.6 nm (0′–1″); (c) $v = 2$ at 248.9 nm (0′–2″). Standard sample conditions are $[N_2O]/[SiH_4]/[H_2]$ = 300/10/3000 mTorr in 10 Torr of He. Special conditions for H_2 and N_2O are indicated in the figure. Thin traces are experiments; solid and dashed smooth lines are numerical simulations when $k_2 = 1.4 \times 10^{-10}$ cm^3 $molecule^{-1}$ s^{-1} and $k_2 = 7.0 \times 10^{-10}$ cm^3 $molecule^{-1}$ s^{-1}, respectively.

The effects of vibrational relaxation of SiO and OH together with their nascent vibrational distributions are also included in the analysis, where the state specific vibrational relaxation rates of SiO were separately measured.[17] It is noted that V-V transfer between SiO(v) and N_2O is predominant for the vibrational relaxation of SiO at the present experimental conditions, whereas contributions from He, H_2, and other components are negligible. The nascent distribution of OH(v) in the reaction of $O(^1D) + H_2$ was taken from our former evaluation.[13] According to the former evaluations on the vibrational relaxation of OH(v),[18,19] it is also the case that N_2O is the predominant collider for the OH(v) relaxation. Assuming the Landau–Teller relation, where $k(v \rightarrow v-1)$ is proportional to v, the OH relaxation rate constants at the collisions with N_2O were fitted so that profiles of OH(0) and OH(1) are well reproduced. The resultant $k(1 \rightarrow 0)$ (4.1×10^{-13} cm^3 $molecule^{-1}$ s^{-1}) is 1.8 times as large as an extrapolation of those obtained at $v \geq 9$ by the direct overtone excitation study,[19] which seems to be within a

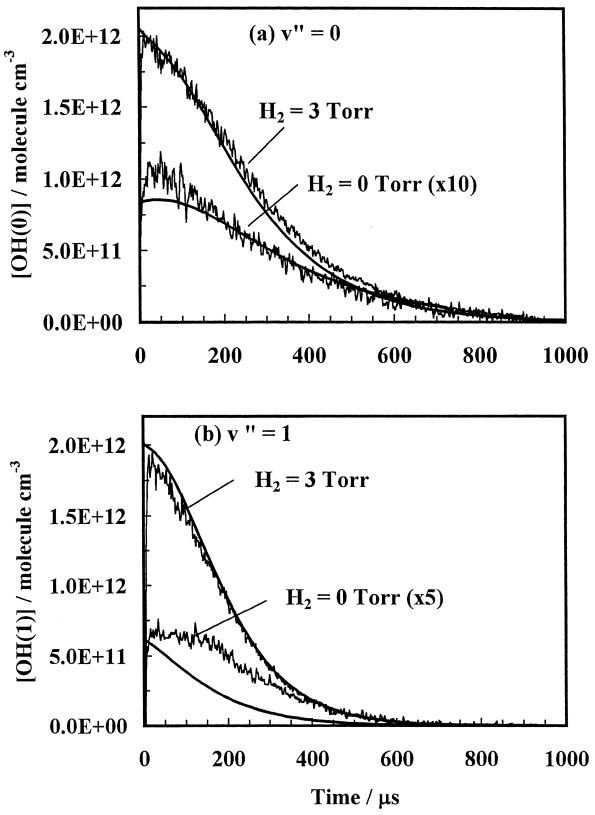

Fig. 2. Time profiles of OH(v) in the 193 nm photolysis of N_2O/SiH_4 mixtures with and without H_2. (a) $v = 0$ probed at 281.92 nm [$(1'–0'')Q_1(1)$ line]; (b) $v = 1$ at 288.24 nm [$(2'–1'')Q_1(1)$]. Standard sample conditions are [N_2O]/[SiH_4] = 300/10 mTorr in 10 Torr He, and H_2 concentrations are indicated in the figure. Thin traces are experiments and solid smooth lines are numerical simulations. Note that vertical scales for samples without H_2 are multiplied by the indicated factors.

reasonable uncertainty.

Finally the diffusion loss rates for SiO and other major products were included in the scheme by fitting the observed long-term decay of the LIF signal intensity.

It was found that the simulated profiles were dominantly governed by the rate constant of (5) rather than that of (2). Specifically, OH profiles could be fitted by adjusting k_5 and OH vibrational relaxation constants. The fitted k_5 (1.27×10^{-11} cm^3 molecule^{-1} s^{-1}) is very close to the literature value (1.23×10^{-11} cm^3 molecule^{-1} s^{-1}).[20] SiO profiles were then further simulated by varying k_2 and ϕ.

Reasonable profiles for SiO(v) were obtained when k_2 is given in the order of 10^{-10} cm^3 molecule^{-1} s^{-1}, as two typical cases are shown in Fig. 1. The higher case (7×10^{-10} cm^3 molecule^{-1} s^{-1}) looks closer to the experimental profile and the lower case (1.4×10^{-10} cm^{3}molecule^{-1} s^{-1}) seems the slower limit of the fit within the experimental fluctuation. Since the higher rate exceeds the collision frequency and it has less sensitivity to the SiO profile, it is considered to be the upper limit. The branching fraction ϕ was given as 0.06 and as 0.18 for higher k_2 and lower k_2, respectively, so that the relative amount of SiO with and without H_2 is reproduced.

The simulated time dependent profiles of OH(v) are mostly in good agreement with those of present observation with and without addition of H_2. The profile of OH(1) in the case without H_2, however, showed a poorer result, probably because the populations of OH at $v > 2$ in the reaction of $SiH_4 + O(^1D)$ are unknown.

Finally total pressure dependence was checked in the range 10–50 Torr (1 Torr $\approx$ 133.322 Pa). No pressure dependence was observed on the SiO yield within experimental uncertainty and the small change in the time profile could be accounted for only by the decreasing rate of diffusion loss with pressure.

Origin of SiO Formation for the Case of Excess H_2. Although the profiles of SiO(v) and OH(v) are reproduced by the simulation, this does not assure that the observed SiO is produced by the reaction of $SiH_3 + OH$ (2). The simulation showed that the profile of SiH_3 is roughly quasi-steady state at the concentration of ca. 5×10^{12} molecule cm^{-3} in the presence of H_2., that is, the condition [SiH_4] $\gg$ [SiH_3] $\gg$ [OH] is attained except during the initial short period (ca. 100 μs) at the photolysis. It is apparent that the decay of OH is predominantly governed by $SiH_4 + OH$ (5) and that reaction (2) acts as a minor perturbation.

With an additional approximation that $O(^1D) + H_2$ (4) is extremely fast, the profiles of OH, H and SiH_3 can be simplified as follows;

$$[OH] = X_0 \exp(-k_5[SiH_4]t) \tag{7}$$

$$[H] = X_0 \exp(-k_6[SiH_4]t) \tag{8}$$

$$[SiH_3] = X_0\{1 - \exp(-k_5[SiH_4]t)\} + X_0\{1 - \exp(-k_6[SiH_4]t)\} \tag{9}$$

where X_0 is the initial concentration of $O(^1D)$, which is proportional to $[N_2O]_0$ when the photolysis yield is constant.

If SiO is produced by (2), its temporal profile is given as;

$$[SiO] = \frac{\phi k_2 X_0^2}{[SiH_4]}\left[\frac{2}{k_5}\{1 - \exp(-k_5[SiH_4]t)\} - \frac{1}{2k_5}\{1 - \exp(-2k_5[SiH_4]t)\} - \frac{1}{k_5 + k_6}\{1 - \exp(-(k_5 + k_6)[SiH_4]t)\}\right]. \tag{10}$$

Alternatively, if SiO is produced by

$$SiH_4 + OH \rightarrow SiO + \text{other products}, \tag{5a}$$

it is simply given as

$$[SiO] = \psi X_0\{1 - \exp(-k_5[SiH_4]t)\}, \tag{11}$$

where $\psi = k_{5a}/k_5$ is the branching fraction for the SiO production in (5). The shapes of (10) and (11) are very close provided that $k_5 \gg k_6$, however, the time dependences of SiO amount on [N_2O] and [SiH_4] are quite different. Our observations with different N_2O and SiH_4 concentrations have supported (10) rather than (11). It is demonstrated in Fig. 1a that [SiO] varies

Table 1. Rate Constants for the Reactions of $SiH_4/N_2O/H_2$ System

No	Reaction	K / cm^3 molecule^{-1} s^{-1}	Branching Fractions	Remark
0	$N_2O + h\nu \rightarrow O(^1D) + N_2$		10^{-3}	photolysis yield
1	$SiH_4 + O(^1D) \rightarrow SiO(v) + 2H_2$ $\rightarrow OH(v) + SiH_3$ $\rightarrow$ other products	3.0×10^{-10} (overall)	0.13 0.36 0.51	Refs. 13, 14
2	$SiH_3 + OH \rightarrow SiO + 2H_2$ $\rightarrow$ other products	$(1.4–7.0) \times 10^{-10}$ (overall)	0.18–0.06[a] 0.82–0.94	this work
3	$O(^1D) + N_2O$	1.16×10^{-10}		b)
4	$O(^1D) + H_2 \rightarrow OH(v) + H$	1.1×10^{-10}		b)
5	$OH + SiH_4 \rightarrow SiH_3 + H_2O$	$(1.27 \pm 0.20) \times 10^{-11}$		this work[c]
6	$H + SiH_4 \rightarrow SiH_3 + H_2$	3.55×10^{-13}		d)

a) Dependent on the assumed overall rate constant. See text.
b) R. Atkinson, D. L. Baulch, R. A. Cox, R. F. Hampson Jr., J. A. Kerr, and J. Tore, *J. Phys. Chem. Ref. Data*, **21**, 1125, (1992).
c) The error limit is given from the scatter range of the fit for different experiments.
d) N. L. Arthur, and T. N. Bell, *Rev. Chem. Intermedt.*, **2**, 37, (1978).*
*New data for $H + SiH_4$ are currently available (e.g. N. L. Arthur, and L. A. Miles, *Chem. Phys. Lett.* **282**, 192 (1998)). The recommended value is still in the middle of the scatter.

with the square of $[N_2O]$.

In addition, the reaction (5a) seems unlikely since it is 45 kJ mol^{-1} endothermic if $2H_2 + H$ is the counterpart products. It is also confirmed in the present numerical simulation that other unidentified secondary products such as SiH_2 or SiH_2O cannot contribute to the high yield of SiO in the presence of H_2. Thus, it is reasonable to conclude that the observed SiO in the photolysis of $N_2O/SiH_4/H_2$ mixture is formed by the $SiH_3 + OH$ reaction.

Nascent Vibrational Distribution of SiO. As described in the previous section, the addition of excess H_2 into SiH_4/N_2O mixture switches the origin of SiO from $SiH_4 + O(^1D)$ into $SiH_3 + OH$, therefore the comparison of SiO formation mechanisms from two different entries is an important task in accordance with the issue of this study. Fluorescence excitation spectra of vibrationally excited SiO have been observed in the wavelength range 226–280 nm in the photolysis of SiH_4/N_2O mixture, where the maximum vibrational quantum numbers that were clearly assigned were 4 and 8 for samples with and without H_2, respectively. The integrated intensities of SiO vibronic bands were translated into relative vibrational populations using Franck–Condon factors and wavelength dependence of the detection system. Small (but non-negligible) corrections for overlapping of different vibrational bands as well as vibrational relaxation were conducted to estimate the nascent vibrational distribution of SiO by using the same method as described in the previous papers.[14,17] In this measurement, the delay time of probe pulse after photolysis was fixed at 20 μs, which is the shortest time within the good S/N condition, while the vibrational relaxation time of $SiO(v)$ is estimated to be 40 μs at this high N_2O concentration. It is noted that the correction for the vibrational relaxation is very minor, since the average time after production of the observed SiO is much shorter than 20 μs at this delay. As shown in Fig. 3, the observed vibrational temperature is approximated to a Boltzmann distribution of $T_v = 2800$ K and 5200 K for samples with and without H_2, respectively.

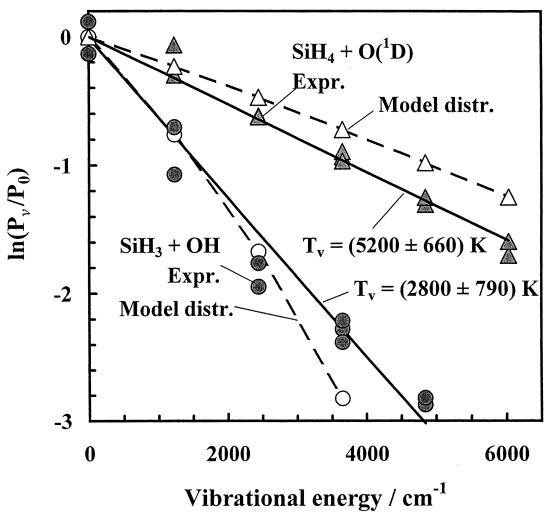

Fig. 3. Nascent distribution of SiO produced by the reactions $SiH_3 + OH$ (circles) and $SiH_4 + O(^1D)$ (triangles). Solid symbols are experiments and Solid lines are linear regressions to the experiments. Dashed curves with open symbols are the Barrier Impulsive Model distributions.

The reaction pathways and resultant vibrational distribution of SiO in the reaction of $SiH_4 + O(^1D)$ have already been discussed in the former paper.[14] The reaction of $SiH_3 + OH$ is considered to have common pathways to the SiO formation with the reaction of $SiH_4 + O(^1D)$, that is, OH and SiH_3 recombine into an activated silanol then redissociate successively as follows

Table 2. Summary of the Calculations of BIM/RRKM Model for the SiO Formation via Unimolecular Decomposition of Activated Silanol Produced in the Reaction of SiH_3 + OH and SiH_4 + $O(^1D)$

Initial reactants	Intermediate(s)	Channel A HSiOH	Channel B H_2SiO	Channel C $H_2SiO \rightarrow$ HSiOH
SiH_3 + OH	Fraction in SiO formation	0.76	0	0.24
	T_v(SiO)/K	2100*	—	2470
SiH_4 + $O(^1D)$	Fraction in SiO formation	0.72	0.06	0.22
	T_v(SiO)/K	5700	2700	5600

a) Populations of v = 0–2 are fitted to the Boltzmann distribution.

$$(H_3SiOH)^* \rightarrow TS1 \rightarrow HSiOH + H_2 \rightarrow TS2 \rightarrow SiO + 2H_2 \quad (A)$$

$$(H_3SiOH)^* \rightarrow TS3 \rightarrow H_2SiO + H_2 \rightarrow TS4 \rightarrow SiO + 2H_2 \quad (B)$$

$$(H_3SiOH)^* \rightarrow TS3 \rightarrow H_2SiO + H_2 \rightarrow TS5 \rightarrow HSiOH + H_2 \rightarrow TS2 \rightarrow SiO + 2H_2 \quad (C).$$

where, the energy diagram is illustrated in Fig. 4. As for other products, H_2SiOH + H and SiH_2 + H_2O are also possible at this energy level.

The product energy distributions are evaluated by means of the barrier impact model (BIM).[14,21] It is assumed in this model that the excess reactant internal energy above TS is statistically partitioned to all the degrees of freedom of the products and that this procedure is repeated in each step passing TS. The results of the calculations are summarized in Table 2. Although all the transition state energies lie below the initial energy level of SiH_3 + OH, the redistributed internal energy of H_2SiO is found to be below TS4; therefore, the contribution of channel C is concluded to be negligible if the calculated energy of TS4 is accepted. The calculated vibrational distribution of SiO through channel A is in reasonable agreement with that of the present experiment as illustrated in Fig. 3. The fraction of SiO through the reaction channel C is minor because of the restriction of the higher energy of TS5. According to the present statistical model, it may be of interest to note that the vibrational energy of SiO via channel C remains higher than that by channel A, since the internal energy is conserved upon isomerization and only the higher part of the internal energy fraction of H_2SiO is transferred to SiO through the isomerization-decomposition of HSiOH. The correlation between the initial reactant energy and the product SiO vibrational temperature is illustrated in Fig. 5, showing that the present statistical model gives a reasonable agreement for the vibrational energy of SiO observed in this study. Consequently, the present study has accounted for the product energy distribution of SiO in the photolysis of SiH_4/N_2O mixture with and without excess H_2 consistently by the mechanism of the multi-step unimolecular decomposition of chemically activated silanol starting at two

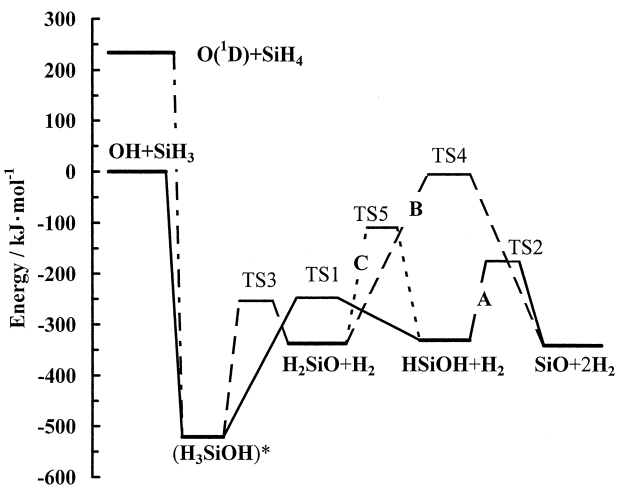

Fig. 4. Energy Diagram for reaction pathways of the multi-step unimolecular decomposition of silanol.

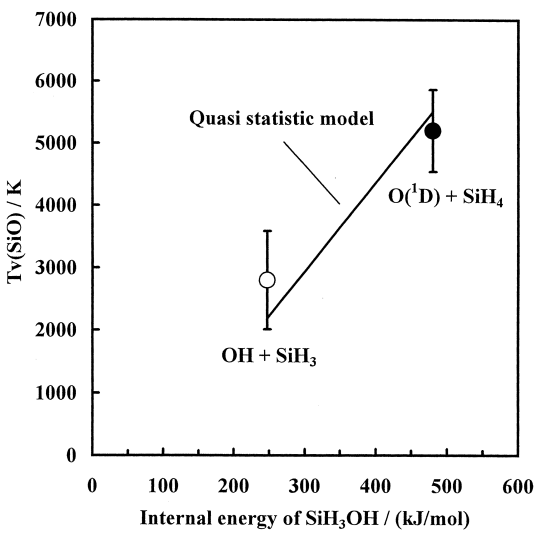

Fig. 5. Vibrational temperature of SiO as a function of internal energy of SiH_3OH prior to dissociation. Points with error bars are present experimental results and the solid line is calculated by BIM model. The model temperature is obtained by averaging the results for possible channels.

different energy levels. On the other hand, the effect of the initial energy of silanol on the yield of SiO would be a further problem. The present evaluation indicated a wide range of the product branching fraction to SiO in the reaction SiH_3 + OH (0.06–0.18) while that in SiH_4 + $O(^1D)$ is in the middle of this range (0.13).

References

1 Y. Murakami, M. Koshi, H. Matsui, K. Kamiya, and H. Umeyama, *J. Phys. Chem.*, **100**, 17501 (1996).

2 M. Koshi, N. Nishida, Y. Murakami, and H. Matsui, *J. Phys. Chem.*, **97**, 4473 (1993).

3 R. W. Quandt and J. F. Hershberger, *Chem. Phys. Lett.*, **206**, 355 (1993).

4 I. R. Slagle, J. R. Bernhardt, and D. Gutman, *Chem. Phys. Lett.*, **149**, 180 (1988).

5 J. R. Hartman, J. Famil-Ghiriha, M. A. Ring, and H. E. O'Neal, *Combust. Flame*, **101**, 170 (1995).

6 M. Koshi, Y. Murakami, and H. Matsui, Modeling of Chemical Reaction Systems, CD-ROM Workshop Proceedings, Heidelberg University (1996).

7 V. I. Babshock, W. Tsang, D. R. Burgess Jr., and M. R. Zachariah, Proceedings of the Twenty-Seventh Symposium (International) on Combustion, The Combustion Institute, Pittsburgh, (1998), p. 2431.

8 M. D. Allendorf, C. Melius, P. Ho, and M. R. Zachariah, *J. Phys. Chem.*, **99**, 15285 (1995).

9 M. R. Zachariah and W. Tsang, *J. Phys. Chem.*, **94**, 5308 (1995).

10 M. S. Gordon and L. A. Perderson, *J. Phys. Chem.*, **94**, 5527 (1990).

11 C. L. Darling and H. B. Schlegel, *J. Phys. Chem.*, **97**, 8207 (1993).

12 A. Tachibana and K. Sakata, *Appl. Surf. Sci.*, **117**, 151 (1997).

13 K. Okuda, K. Yunoki, T. Oguchi, Y. Murakami, A. Tezaki, M. Koshi, and H. Matsui, *J. Phys. Chem. A*, **101**, 2365 (1997).

14 A. Takahara, A. Tezaki, and H. Matsui, *J. Phys. Chem. A*, **103**, 11315 (1999).

15 J. J. Lin, Y. T. Lee, X. Yang, *J. Chem. Phys.*, **113**, 1831 (2000).

16 W. Hack and H. Tiesemann, *J. Phys. Chem.*, **99**, 17364 (1995).

17 A. Takahara, A. Tezaki, and H. Matsui, *Bull. Chem. Soc. Jpn*, **73**, 801 (2000).

18 K. J. Rensverger, J. B. Jeffries, and D. R. Crosley, *J. Chem. Phys.*, **90**, 2174 (1989).

19 A. D. Sappey and R. A. Copeland, *J. Chem. Phys.*, **93**, 5741 (1990).

20 R. Atkinson and J. N. Pitts Jr., *Int. J. Chem. Kintet.*, **10**, 1151 (1978).

21 S. W. North, D. A. Blank, J. D. Gezelter, C. A. Longfellow, Y. T. Lee, *J. Chem. Phys.*, **102**, 4447 (1995).